The microwave spectrum of HO_2 near 65 GHz*

Yardley Beers

National Bureau of Standards, Boulder, Colorado 80302

Carleton J. Howard

Aeronomy Laboratory, NOAA Environmental Research Laboratories, Boulder, Colorado 80302
(Received 16 June 1975)

Using a Zeeman-modulated cavity spectrometer with a 10 sec time constant and a phase locked klystron, we have observed in the products of a discharge-flow system, Zeeman components of the six allowed zero-field lines at 65070±2, 65082±2, 65098±2, 65373±2, 65397±2, and 65401±2 MHz, and of one forbidden zero-field line at 65369±4 MHz. The Q of the Fabry–Perot cavity is about 10000, and the magnetic field was swept from 0–30 G. Chemical tests indicate that the observed lines are due to HO_2. They have been assigned and least-squares fitted using a simple theoretical model to yield a value of 65185±2 MHz for the 1_{01}–0_{00} asymmetric rotor transition frequency of HO_2, a value of −208±2 MHz for the linear combination $(\epsilon_{bb}+\epsilon_{cc})/2$ of elements of the electron spin–molecular rotation interaction tensor, a value of −28±2 MHz for the nuclear spin–electron spin Fermi contact interaction parameter σ, and a value of +4±2 MHz for the spin–spin tensor interaction parameter λ. These constants are in excellent agreement with three less precise constants obtained from an earlier laser magnetic resonance study and have been confirmed by recent more accurate measurements of Saito.

I. INTRODUCTION

The matrix isolation infrared spectrum[1,2] as well as the gas phase ultraviolet absorption spectrum[3,4] near infrared absorption[5] and emission[6] spectrum, and far infrared laser magnetic resonance spectrum[7–9] of the HO_2 free radical can now all be found in the literature. In the present paper we report the first microwave detection of HO_2, with an analysis of the Zeeman splittings of the fine and hyperfine structure of the asymmetric rotor transition $N_{K_aK_c} = 1_{01} \leftarrow 0_{00}$.

The values of the rotational constants and spin–rotation splitting constants obtained earlier[9] aided in limiting the microwave search problem and made convenient the use of a Zeeman-modulated cavity spectrometer. Similarly, the chemical production methods developed[7] could be employed essentially without change for the small volume cavity cell.

The errors in individual measurements in the present work sometimes exceed several gauss, or equivalently, several MHz. They presumably arise (i) from pressure broadening in the 0.1–0.2 torr gas flow mixtures, (ii) from inhomogeneities in the magnetic field of the von Helmholtz coils across the relatively large sample cell, and (iii) from cavity pulling effects associated with a high-Q cavity containing a dielectric sample cell. Even though errors of several MHz are somewhat larger than is customary in microwave studies in the 65 GHz region, the present measurements lead to a factor of 1000 improvement in the error limits on the 1_{01}–0_{00} transition frequency predicted earlier.[9]

II. EXPERIMENTAL

A. Apparatus

This experiment employed a Zeeman-modulated cavity spectrometer. Figure 1 shows a simplified sketch of the equipment. The HO_2 radicals are produced by a discharge–flow system in a quartz bottle contained between the plane plates of a Fabry-Perot resonator, which is located inside von Helmholtz coils. Power from a klystron is fed through a directional coupler to the entrance iris of the resonator, where some of the power is reflected to the detector. This enhances the sensitivity by heterodyne action. The arm of the directional coupler, which in Fig. 1 is shown as being terminated by a sliding short circuit, actually goes to an extensive microwave circuit, which provides for the phase locking of the V-band klystron to the harmonic of an X-band klystron, which in turn is phase locked to a harmonic of a quartz crystal controlled oscillator. The frequency of the quartz crystal oscillator, of the if oscillators, and of the variable frequency interpolation oscillator contained in the two phase locking loops were measured with a counter. From these measurements the frequency of the V-band klystron was calculated. By inserting a 90° waveguide twist to rotate the microwave polarization, both π and σ Zeeman components were observed.

In an era in which the confocal Fabry-Perot interferometer is widely used, some words justifying the parallel plate Fabry-Perot configuration are in order. It has been shown[10] that the signal to noise ratio of a cavity spectrometer with the power adjusted to the verge of saturation is

$$S = (hc\gamma f/8\pi\mu)(\Delta\nu/\nu)(QV\nu/2FkTB)^{1/2}\,, \qquad (1)$$

where γ is the absorption coefficient of the sample, f is the fraction of volume V occupied by sample, μ is the dipole matrix element of transition, $\Delta\nu$ is the linewidth parameter, ν is the frequency of the transition, Q is the quality factor of the loaded resonator, V is the volume of the resonator, F and B are the noise figure and noise bandwidth of the detection system with a reference temperature T, and h, c, and k have their usual meanings.

In the original derivation of Eq. (1) it was assumed that the sample filled the entire volume and f was unity. However, when f is less than 1, its effect is to reduce the average value of γ to $f\gamma$ without affecting other steps in the derivation.

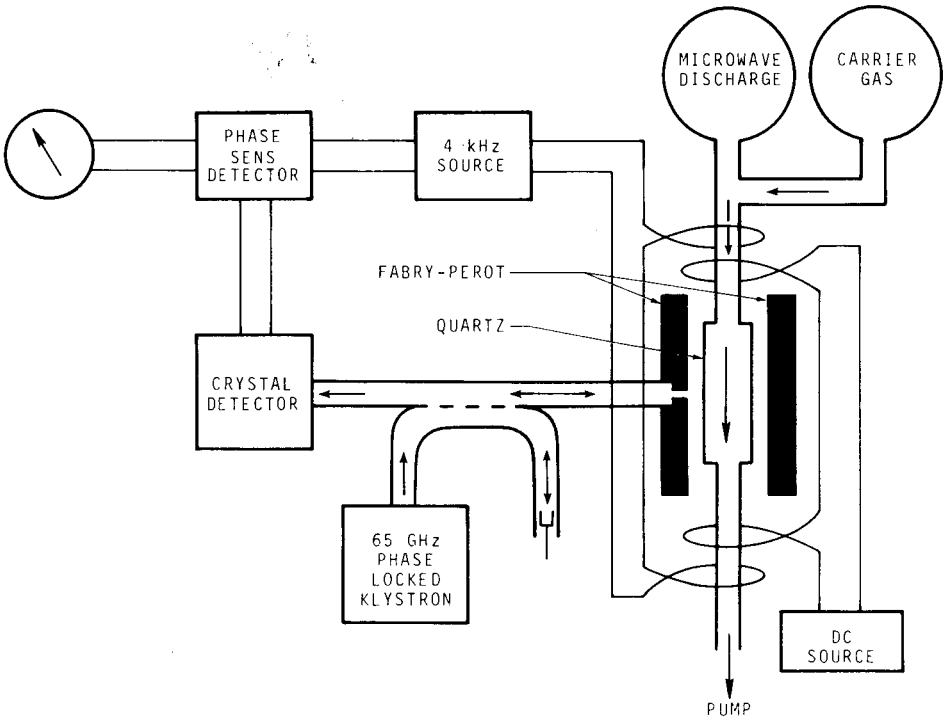

FIG. 1. Simplified schematic diagram of the apparatus. The waveguide port of the directional coupler, which is shown as being terminated by a sliding short circuit, goes in the actual apparatus to an extensive microwave circuit that provides for the phase locking of the klystron. The von Helmholtz coils, shown with axis along the gas flow direction, actually have their axis perpendicular to the plane of the figure.

For a parallel plate Fabry-Perot resonator, whose only losses are due to the finite conductivity of the plates of reflectance, R, and whose spacing is L, the unloaded Q is given by[11]

$$Q = 2\pi L\nu/[c(1-R)] . \quad (2)$$

Equation (2) contains the approximation that R is nearly unity. It should hold approximately for confocal resonators as well, provided that diffraction can be neglected. As a further approximation, we may neglect the difference between loaded and unloaded Q and substitute Eq. (2) into Eq. (1). Also, we set the volume $V = AL$, where A is the effective area of cross section. If the quartz container for our sample has parallel plane sides of negligible thickness and separation x, $f = x/L$. Then

$$S = (h\gamma x\Delta\nu/8\pi\mu)[\pi cA/(1-R)FkTB]^{1/2} . \quad (3)$$

We note that this result is independent of the resonator length L.

The previous discussion has assumed no diffraction losses, and if these are considered, it is obvious that the optimum spacing L is the minimum that can conveniently contain the sample cell of thickness x. With a large cross section A and small spacing x, the curvature required for the *confocal* configuration cannot be obtained under practical conditions. Furthermore, if the plates are plane they may be used to produce a moderately uniform Stark field under appropriate conditions.

The resonator was used in an earlier experiment[12] but has been modified. In the original version, the resonator was contained in a vacuum chamber, and the coupling to the microwave circuit was with a horn and grid arrangement using a window in the chamber. In the present configuration, the vacuum chamber was discarded because of the use of the quartz bottle, and the screen containing the grid of holes is replaced by a solid plate with a single iris. A piece of RG-138/U waveguide is mounted coaxially with this iris.

In the original design, the spacing and the degree of parallelism were controlled independently, and with the tilt controls on the plates, the task of making the plates parallel was very small, requiring only a minute or two. With the rigid attachment of the waveguide to one plate, one of the tilt controls had to be discarded, but with the aid of a small amount of shimming and with the use of the surviving tile control, the adjustment for parallelism is still a minor task.

The plates are made of quarter-inch brass and they have diameters of about 35 and 18 cm, respectively. Polishing and gold plating were found to be crucial for obtaining a high Q. During the experiment, the spacing was about 6 cm. The coupling hole size was found by trial and error. The present hole is roughly elliptical in shape, with the minor axis nearly equal to the short dimension of the RG-138/U waveguide (0.1 cm). With the presence of several sets of mounting holes at the periphery of the plate, a variation in coupling coefficient can be obtained by rotating the plate about the waveguide axis.

The quartz absorption cell is 8 cm in diameter and has approximately parallel plane sides 4 cm apart with a wall thickness of about 0.3 cm. The principal support of the quartz assembly is a clamp at the bottom. However, this support is not completely rigid, and the position of the upper portion can be controlled by the clamp at the top. This clamp is supported by a micrometer drive, which acts as a fine control on the position of the quartz assembly in the resonator. The rough position of the assembly can be varied by adjusting the bottom clamp.

The performance of the resonator depends critically upon the position of the quartz assembly. If the cell is not in roughly the right position, it is difficult to observe any resonance, and for optimum performance it is necessary to readjust the micrometer when the frequency is shifted. Culshaw and Anderson[13] have shown that the performance of a Fabry-Perot resonator with a slab of dielectric in it depends upon the slab position unless it happens to be an integral number of half-wavelengths thick. Also, it was found necessary to have an air gap of about 1 cm between the plate containing the iris and the quartz. With the quartz present and with the system in optimum adjustment, the loaded Q is in excess of 10 000, corresponding to a path length in the sample of several meters according to Ref. 10. Generally, it is impractical to achieve such path lengths with transient molecules in traveling wave cells. On the other hand, with the comparatively high gas pressures used in this experiment, the bandwidth of the cavity is hardly any larger than the linewidth.

The average dimensions of the von Helmholtz coils are 15×28 cm, and the average spacing is 25 cm. Each has a winding of 500 turns of No. 18 wire which is used to supply a dc field, and another winding of 300 turns which is connected to a 4 KHz sine wave source for modulation, making phase sensitive detection possible. Unfortunately, the coils were not designed to be mounted vertically, which would have permitted annulling the major component of the earth's field. But this error is not serious, since the earth's field (~ 0.8 G) corresponds to less than a linewidth. The axis of the coils is nearly perpendicular to the horizontal component of the earth's field, but a correction to the data is applied to compensate for the portion that is parallel to the axis.

Because of the narrow bandwidth of the cavity, it is not practical to obtain useful data by sweeping the frequency. Instead the procedure is to set the phase locked klystron to some selected frequency, resonate the cavity, including readjustment of the micrometer controlling the position of the quartz cell, and then sweep the magnetic field. The field could be swept from 0–33 G. Normally the modulation field is 0.5 G rms. With the present apparatus it is not practical to observe zero-field unsplit lines or field-independent Zeeman components.

The primary measurement associated with the magnetic field sweep was in fact a measurement of the voltage across the von Helmholtz coils. Normally, the voltage was measured with a digital voltmeter, but this reading was checked against the calibration of the xy recorder being used. The resistance of the coils was measured with a Wheatstone bridge. Values of the magnetic field were then determined from the calculated current flow and the geometry. Several fields were checked using a magnetometer, and the error in field measurement is estimated to be $\pm 5\%$.

Pulling effects of the resonator are a major source of error. To evaluate some of the errors, two Zeeman components were first observed a number of times as rapidly as possible without making any readjustments. The standard deviation was 0.04 G. Then, for several days, the same components were observed once a day, and each day the microwave system was drastically detuned and then readjusted for optimum. The standard deviation was found to be 0.22 G, nearly 6 times as large.

A preliminary check of the sensitivity of the system was made using transitions of CH_3CN in the same frequency region. For this purpose a Stark field was applied between the Fabry-Perot plates. While modulation was effective and while resolved Stark components could be observed, quantitatively the results were not reproducible, probably because of erratic charge distributions on the quartz absorption cell.

All of the lines reported in the present work should exhibit only quadratic Stark effects. A couple of sample lines were subjected to a dc Stark field of 650 V/cm, and no effects were observed, indicating that, in accordance with expectations, they are not subject to the first order Stark effect.

B. HO_2 source chemistry

HO_2 radicals were generated inside the quartz absorption cell using chemical methods similar to those described earlier.[7] The optimum flow and pressure conditions for maximum HO_2 concentrations and minimum pressure broadening in the microwave experiment were found using a laser magnetic resonance apparatus.

Three different chemical schemes were used to demonstrate that HO_2 was detected.

(i) The most prolific source of HO_2 was the reaction of atomic fluorine with hydrogen peroxide. The atomic fluorine was generated in an alumina lined Pyrex discharge tube using an electrodeless 2450 MHz cavity. A mixture of about 2.7 Pa (1 mm Hg = 133.3 Pa) of air with about 11 Pa of CF_4 was discharged and pumped through a 36 cm length of 6.35 mm o.d. Teflon tubing to the entrance of the quartz absorption cell. At this point, the discharged gas was mixed with about 5.4 Pa of H_2O_2 vapor, allowing HO_2 to be formed in the absorption cell by the reaction

$$F + H_2O_2 \rightarrow HO_2 + HF. \quad (4)$$

This source produced excellent signals, with a typical signal to noise ratio of about 40 to 1 for a strong line as shown in Fig. 2.

(ii) A second source, the chain reaction of active oxygen with ethylene, was about 10 times weaker. Atomic oxygen was formed by discharging about 2.7 Pa of O_2. The atomic oxygen was then mixed with about 13 Pa of O_2 and 5.4 Pa of C_2H_4 in the absorption cell, forming HO_2 by the reactions

$$O + C_2H_4 \rightarrow HCO + CH_3 \text{ and } HCO + O_2 \rightarrow HO_2 + CO. \quad (5)$$

(iii) A third source, also about 10 times weaker than (i), was allyl alcohol. Although the mechanism of HO_2 formation in this case is not known, replacing the C_2H_4 in (ii) with allyl alcohol was a strong source of HO_2 in the laser magnetic resonance spectrometer. Unfortunately, this source was relatively much weaker in the microwave experiment, possibly due to differences in pumping speed or radical destruction rates on the ab-

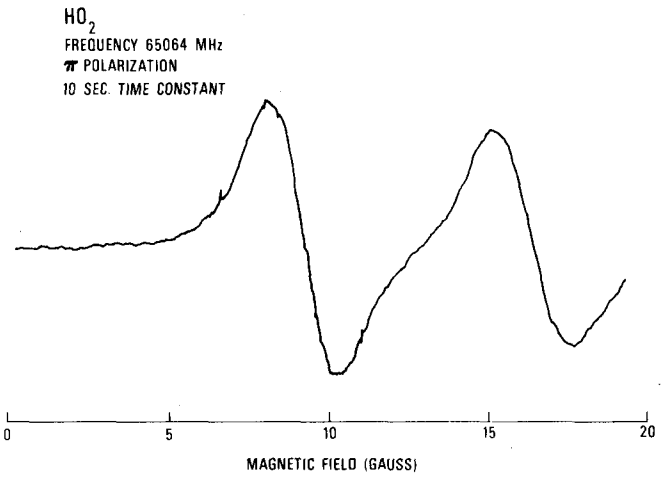

FIG. 2. A representative recording of two Zeeman components.

sorption cell walls of the two systems.

In addition to using three different known sources, we made several tests on each source to demonstrate that the mechanisms outlined above were responsible for the production of HO_2 rather than some other paramagnetic molecule. First, it was shown that the discharge that forms atomic fluorine, source (i), or atomic oxygen, sources (ii) and (iii), had to be turned on for a signal to be observed. Further, the air used in source (i) could be eliminated without eliminating the signal, although, some H_2O_2 vapor was required. Both sources (ii) and (iii) required hydrocarbon vapor to produce signals. These tests eliminate carbon, nitrogen, oxygen, and silicon (from glassware) fluorides, ground state and metastable molecular oxygen, and carbon–oxygen compounds as potential sources of the detected signal. Three molecules, O_2, [14] SiF_2, [15] and CF_2 [16] can also be neglected, since their microwave spectra are known not to have lines at the frequencies reported here. These considerations, combined with the results of the analysis that follows, firmly demonstrate that HO_2 is the detected species.

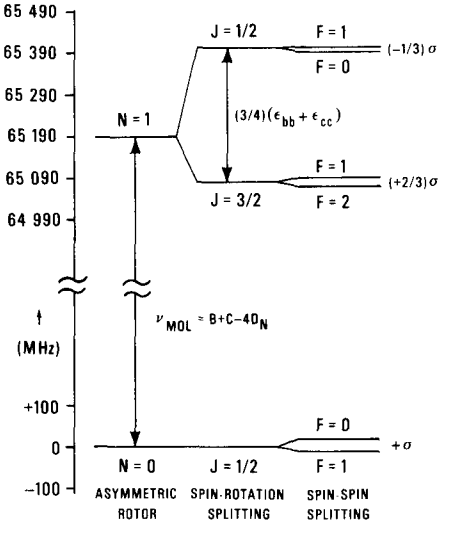

FIG. 3. Illustration for the molecule HO_2 of the 1_{01}–0_{00} rotational energy level separation ν_{mol}, the spin–rotation fine-structure splitting $(\frac{3}{4})(\epsilon_{bb}+\epsilon_{cc})$, and the spin–spin hyperfine splittings.

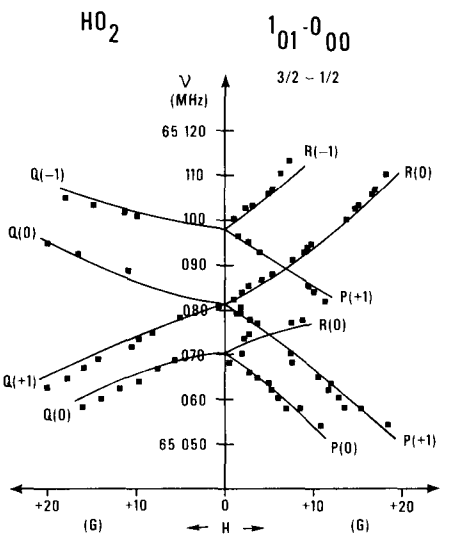

FIG. 4. HO_2 transition frequencies near 65 100 MHz as a function of the external magnetic field H. The squares represent observed points, the smooth curves represent calculated values obtained from a least-squares fit of these points using Eqs. (6). These transitions correspond, from higher energy to lower, to $(N'=1,\ J'=\frac{3}{2},\ F'=1,2,1)$–$(N''=0,\ J''=\frac{1}{2},\ F''=1,1,0)$, respectively. The notation $P(M_F)$, $Q(M_F)$, $R(M_F)$ indicates transitions with $\Delta M_F=-1,0,+1$, originating from a lower state level with the M_F value given in parentheses. Note that the parallel spectrum is plotted to the left of center, the perpendicular spectrum to the right. Molecular parameters obtained from the least squares fit are given in Table I.

III. RESULTS

The quantum numbers of interest in this work are the rotational angular momentum N; the electron spin an-

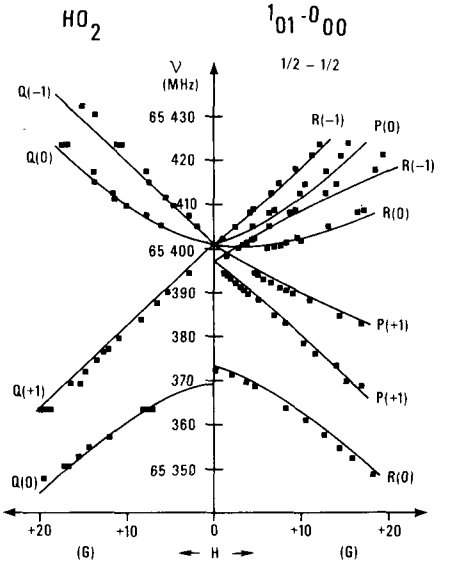

FIG. 5. HO_2 transition frequencies near 65 400 MHz, displayed as in Fig. 4, and corresponding, from higher energy to lower, to $(N'=1,\ J'=\frac{1}{2},\ F'=1,0,1,0)$–$(N''=0,\ J''=\frac{1}{2},\ F''=1,1,0,0)$, respectively.

TABLE I. Molecular parameters ν_0, σ', σ'' and standard deviation of the fit σ_{fit} in MHz, as obtained directly from least-squares fits of the observed data in Figs. 4 and 5 to Eqs. (6). Errors represent one standard deviation.

	$(J'=\frac{3}{2}) \leftarrow (J''=\frac{1}{2})$	$(J'=\frac{1}{2}) \leftarrow (J''=\frac{1}{2})$
ν_0	65 080.83 ± 0.17	65 393.16 ± 0.13
σ'	−24.80 ± 0.64	−12.0 ± 1.2
σ''	−28.12 ± 0.50	−27.86 ± 0.40
σ_{fit}	1.42	1.47

gular momentum S; the sum of these two, J; the proton spin angular momentum I; and the total angular momentum, F. These quantum numbers are illustrated in Fig. 3. It can be shown that energy levels of HO_2 in the presence of a small external magnetic field (≤ 20 G), which arise from a given spin–rotational level with fixed N and J, are well approximated by the expressions

$$E = \nu_0 + X(g\mu_B H M_F - \tfrac{1}{4}\sigma) + \tfrac{1}{2}X(g\mu_B H - \sigma M_F), \quad (6a)$$

$$E = \nu_0 + X(g\mu_B H M_F - \tfrac{1}{4}\sigma) \pm \tfrac{1}{2}X[\sigma^2(J+\tfrac{1}{2})^2 - 2\sigma g\mu_B H M_F + g^2\mu_B^2 H^2]^{1/2}, \quad (6b)$$

$$E = \nu_0 + X(g\mu_B H M_F - \tfrac{1}{4}\sigma) - \tfrac{1}{2}X(g\mu_B H - \sigma M_F), \quad (6c)$$

for $M_F = -(J+\frac{1}{2})$, $|M_F| \leq (J-\frac{1}{2})$, and $M_F = +(J+\frac{1}{2})$, respectively. Here, ν_0 indicates the rotational and spin–rotational energy of the given N, J level; X represents $[J(J+1) - N(N+1) + S(S+1)]/2J(J+1)$; g is the free electron gyromagnetic ratio; μ_B is the Bohr magneton in MHz/G; H is the external magnetic field gauss; M_F is the projection of the total angular momentum along the external field direction; and σ is an effective electron spin–proton spin interaction parameter in MHz.

Observed transition frequencies as a function of magnetic field are displayed as solid squares in Figs. 4 and 5, respectively, for the $(N=1,\ J=\frac{3}{2})$–$(N=0,\ J=\frac{1}{2})$ and $(N=1,\ J=\frac{1}{2})$–$(N=0,\ J=\frac{1}{2})$ transitions. Solid rectangles indicate the scatter obtained in several measurements of essentially the same point. Back calculated theoretical curves obtained by a separate least-squares fit of the data in each figure to energy differences obtained from Eqs. (6) are indicated by solid curves. Parameters obtained from the fits are given in Table I. Note that for clarity, parallel polarization observations are plotted to the left of center in Figs. 4 and 5 and perpendicular polarization observations to the right.

From the least-squares parameters in Table I it is possible to calculate the four molecular parameters given in Table II. It can be seen that our numbers agree well with the more recent precise numbers obtained by Saito[17] in a conventional microwave study. The constants $B+C$ and $\frac{1}{2}(\epsilon_{bb}+\epsilon_{cc})$ also agree well (within 10 MHz) with the values obtained in an earlier laser magnetic resonance study.

TABLE II. Values in MHz of the molecular parameters for HO_2 illustrated in the energy level diagram of Fig. 3.

Parameter	Hougen *et al.*[9]	Saito[17]	This work
$(B+C)$	65 190 ± 1500	65 185.40 ± 0.11	65 185 ± 2
$\frac{1}{2}(\epsilon_{bb}+\epsilon_{cc})$	−216 ± 18	−207.15 ± 0.12	−208 ± 2
σ		−27.61 ± 0.14 (A_F)	−28 ± 2
λ		+4.1 ± 0.2 $(-\frac{1}{2}T_{aa})$	+3.6 ± 2

TABLE III. Zero-field transition frequencies as determined by the present work, in MHz.

$N'J'F'-N''J''F''$	$\nu_{\text{zero field}}$
$1\,\frac{1}{2}\,1-0\,\frac{1}{2}\,1$	65 401 ± 2
$1\,\frac{1}{2}\,0-0\,\frac{1}{2}\,1$	65 397 ± 2
$1\,\frac{1}{2}\,1-0\,\frac{1}{2}\,0$	65 373 ± 2
$1\,\frac{1}{2}\,0-0\,\frac{1}{2}\,0$	65 369 ± 4 (forbidden)
$1\,\frac{3}{2}\,1-0\,\frac{1}{2}\,1$	65 098 ± 2
$1\,\frac{3}{2}\,2-0\,\frac{1}{2}\,1$	65 082 ± 2
$1\,\frac{3}{2}\,1-0\,\frac{1}{2}\,0$	65 070 ± 2

Table III gives the frequencies of the zero-field transitions according to the energy levels shown in Fig. 3.

ACKNOWLEDGMENTS

We are greatly indebted to Dr. J. T. Hougen for providing an invaluable analysis and assignment of the HO_2 spectrum. We also thank Dr. K. M. Evenson for helpful discussions and Dr. S. Saito for allowing us to refer to his prepublication results. This work was supported in part by the National Bureau of Standards Office of Air and Water Measurements.

*A preliminary report of this work was given at the Thirtieth Symposium on Molecular Structure and Spectroscopy, Ohio State University, Columbus, Ohio, June 17, 1975.
[1]D. E. Milligan and M. E. Jacox, J. Chem. Phys. **38**, 2627 (1963).
[2]M. E. Jacox and D. E. Milligan, J. Mol. Spectrosc. **42**, 495 (1972).
[3]T. T. Paukert and H. S. Johnston, J. Chem. Phys. **56**, 2824 (1972).
[4]C. J. Hochanadel, J. A. Ghormley, and T. J. Ogren, J. Chem Chem. Phys. **56**, 4426 (1972).
[5]H. E. Hunziker and H. R. Wendt, J. Chem. Phys. **60**, 4622 (1974).
[6]K. H. Becker, E. H. Fink, P. Langen, and H. Schurath, J. Chem. Phys. **60**, 4623 (1974).
[7]H. E. Radford, K. M. Evenson, and C. J. Howard, J. Chem. Phys. **60**, 3178 (1974).
[8]J. T. Hougen, J. Mol. Spectrosc. **54**, 447 (1975).
[9]J. T. Hougen, H. E. Radford, K. M. Evenson, and C. J. Howard, J. Mol. Spectrosc. **56**, 210 (1975).
[10]Y. Beers, Rev. Sci. Instrum. **30**, 9 (1959).
[11]W. Culshaw, IRE Trans. Microwave Theory Tech. **MIT-9**, 135 (1961).
[12]Y. Beers and T. W. Russell, IEEE Trans. Instrum. Meas. **IM-15**, 380 (1966).
[13]W. Culshaw and M. V. Anderson, Proc. Inst. Electr. Eng. Part B Suppl. **109**, 820 (1962).
[14]W. M. Welch and M. Mizushima, Phys. Rev. A **5**, 2692 (1972).
[15]V. M. Rao, R. F. Curl, P. L. Timms, and J. L. Margrave, J. Chem. Phys. **43**, 2557 (1965).
[16]F. X. Powell and D. R. Lide, J. Chem. Phys. **45**, 1067 (1966).
[17]S. Saito (private communication).